Hindawi
Journal of Chemistry
Volume 2019, Article ID 2678927, 7 pages
https://doi.org/10.1155/2019/2678927

Research Article

Novel Removal of Diazinon Pesticide by Adsorption and Photocatalytic Degradation of Visible Light-Driven Fe-TiO_2/Bent-Fe Photocatalyst

Nguyen Minh Phuong,[1] **Ngoc Chau Chu**,[1] **Doan Van Thuan**,[2] **Minh Ngoc Ha**,[1] **Nguyen Thi Hanh**,[3] **Huong Do Thi Viet**,[1] **Nguyen Thi Minh Thu**,[1] **Pham Van Quan**,[4] **and Nguyen Thi Thanh Truc**[5]

[1]*Faculty of Chemistry, University of Science, Vietnam National University, 334 Nguyen Trai, Thanh Xuan, Hanoi, Vietnam*
[2]*NTT Hi-Tech Institute, Nguyen Tat Thanh University, Ho Chi Minh City 700000, Vietnam*
[3]*Faculty of Environmental Science, University of Science, Vietnam National University, 334 Nguyen Trai, Thanh Xuan, Hanoi, Vietnam*
[4]*Ministry of Industry and Trade, 54 Hai Ba Trung, Hoan Kiem, Hanoi, Vietnam*
[5]*Faculty of Environment and Labour Safety, Ton Duc Thang University, Ho Chi Minh City, Vietnam*

Correspondence should be addressed to Nguyen Minh Phuong; nguyenminhphuong@hus.edu.vn

Received 11 December 2018; Revised 26 January 2019; Accepted 13 February 2019; Published 20 March 2019

Guest Editor: Ajit Kumar Sharma

In the study, Fe was used as a dopant to enhance photocatalytic activity of TiO_2. Then, the Fe-doped TiO_2 was deposited on bentonite, which was pillared by Fe. The synthesized materials were characterized by SEM, XRD, UV-Vis, BET, and point of zero charge (pH_{PZC}). Then, the synthesized materials were used for diazinon removal under both dark and visible light conditions to investigate adsorption and photocatalytic degradation abilities of the synthesized materials. The maximum diazinon adsorption capacity of the synthesized Fe-TiO_2/Bent-Fe was 27.03 mg/g. The obtained results indicated that the Fe-TiO_2/Bent-Fe exhibited high photocatalytic degradation activity for removal of diazinon even under visible light. The diazinon removal experiments were also conducted using different photocatalyst dosages, under different pH and light sources to figure the optimal conditions for removal processes. The obtained results indicated that optimal photocatalyst dosage and pH were 0.5 g/L and 4.5, respectively. Finally, the natural light generated from solar could be suitable used for diazinon removal by the synthesized Fe-TiO_2/Bent-Fe.

1. Introduction

Many kinds of pesticides releasing into the environment as a result of runoff from agricultural and urban areas cause pollution of soil, air, surface water, and groundwater and are harmful for the human health [1, 2]. Among them, diazinon (*O*, *O*-diethyl *O*-[6-methyl-2-(1-methylethyl)-4-pyrimidinyl] phosphorothioate), an organophosphorus and highly toxic pesticide, is extensively used to control insects and, just in the USA, 6 million pounds of the pesticide are annually used on farming sites [3]. The diazinon has been classified as moderately hazardous class II chemical to humans, aquatics, mammals, and other species by the World Health Organization (WHO). Shemer and Linden reported that the fatal human doses of diazinon were in the range from 90 to 444 $mg{\cdot}kg^{-1}$ [4]. Kouloumbos et al. reported that toxic effects of the pesticide attributed to its inhibition of the enzyme acetylcholinesterase affecting the nervous system [5]. Therefore, water systems contaminated with diazinon have been treated by various techniques such as adsorption, filtration, membrane separation, biodegradation, oxidation, and chemical coagulation [6]. However, these methods have several certain disadvantages including incomplete removal, high consumption of chemicals, time consuming, and high treatment cost.

Recently, advanced oxidation processes (AOPs), using heterogeneous photocatalysts to produce hydroxyl radicals ($^*OH$), a strong oxidative agent, to totally promote mineralization of organic pollutants into harmless substances such as CO_2 and H_2O, could be a potential technology for removal of diazinon [7–9]. Titanium oxide (TiO_2) is regarded as the most suitable photocatalyst for the degradation of organic pollutants from wastewaters because of its chemical stability, nontoxicity, low cost, and commercial availability [10–12]. However, because of wide band gap of TiO_2, which is approximately 3.2 eV, the photocatalyst could only be activated by UV irradiation, which only accounts for 3-4% of the solar spectrum [13, 14]. The high-energy consumption and safety issues concerning use of UV irradiation are the main disadvantages of TiO_2 in the practical system. In addition, the fast recombination of the photoexcited electrons and holes is also another disadvantage of the TiO_2 photocatalyst. Hence, numerous studies have been conducted to effectively enhance the photocatalytic activity of TiO_2 and to expand its applications in practical systems using visible light or the solar energy as the excitation source [15–21]. Among these, metals have been used as doping agents to implant or incorporate into the TiO_2 lattice to narrow the band gap of the photocatalyst, thereby enhancing its photocatalytic activity [22–27]. The overlap between d orbital of the substituted metal and d orbital of titanium could narrow band gap or facilitate the visible light absorption of the doped TiO_2, leading to its photocatalytic enhancement [28]. Therefore, the first aim of the study is to use Fe as dopant to enhance photocatalytic activity of TiO_2 to utilize visible light as excitation sources for its photocatalytic removal of diazinon.

In addition, it is difficult to recover powder photocatalysts after being used in practical system for wastewater treatment. Moreover, the photocatalytic activity of a certain photocatalyst strongly depends on its adsorption capacity [29]. Various materials including activated carbon, glass fiber, polyurethane, silica, alumina, and bentonite have been used as supports to fix photocatalysts to overcome such limitations. In the study, bentonite, which is nontoxic, porous, economical, easily available in our country (Vietnam), and also chemically and mechanically stable, was used as support materials for Fe-doped TiO_2 (Fe-TiO_2). However, the surface area of the natural bentonite is quite small. Many studies reported that the introduction of the inorganic pillars into bentonite could increase its surface area, pore volume, microporosity, and thermal stability [30–32]. Therefore, the study used Fe as a pillar to increase surface area as well as pore volume of the bentonite before being used as support for the Fe-TiO_2. Thus, the Fe-doped TiO_2 supported on bentonite pillared Fe (Fe-TiO_2/Bent-Fe) would have high photocatalytic activity and adsorption capacity for removal of diazinon.

2. Experimental

2.1. Material Preparation. First, 10 g bentonite was saturated with Fe^{3+} in 100 mL of 1 M solution of $FeCl_3$ under constant stirring. The obtained suspension was continuously stirred at room temperature for 24 h. The resulting product was centrifuged and washed by distilled water until chloride free (tested by $AgNO_3$). The obtained material was dried at 363 K for 12 h and then milled to get bentonite-pillared Fe (Bent-Fe). Then, the obtained Bent-Fe was swelled in pure ethanol solution with weight ratio of 2%. Second, 6 mL tetra isopropyl orthotitanate (TIOT) was slowly dropped into 34 mL ethanol to get a solution "A" while 48.2 mg $Fe(NO_3)_3{\cdot}9H_2O$ was diluted in a solution containing 17 mL ethanol, 0.4 mL HNO_3 (68%), and 1.6 mL distilled water to obtain a solution "B". Then, the solution "A" was slowly dropped into the solution "B" to get sol Fe-TiO_2. Finally, the obtained sol Fe-TiO_2 was slowly dropped into the swelled Bent-Fe with continuously stirring for 4 h and aging for 24 h. The obtained mixture was changed into a Teflon-lined stainless steel autoclave and then heated under 160°C for 6 h. After the autoclave was cooled to room temperature, the precipitate at the bottom of the autoclave was obtained and washed with ethanol and deionized water several times. The product was dried at 80°C for 24 h to get Fe-TiO_2/Bent-Fe. The weight ratio of (Fe-TiO_2)/(Bent-Fe) was 3 : 1.

2.2. Photocatalyst Characterization. The surface morphology of the synthesized materials was analyzed using a JED-2300-Analysis Station Plus, JEOL scanning electron microscope (SEM). X-ray diffraction (XRD) spectra of the synthesized TiO_2, Fe-TiO_2, Fe-TiO_2/Bent, Bent-Fe, and Fe-TiO_2/Bent-Fe materials were obtained using a D8-Advance 5005 model with Cu-Kα ($\lambda = 1.5406$ Å) radiation over the range $10^\circ < 2\theta < 70^\circ$, at a scanning rate of 0.03°/min. The optical absorption abilities of the synthesized photocatalysts were characterized by an UV 3101PC spectrophotometer, Shimadzu. The point of zero charge (pH_{PZC}) of the synthesized material was determined using the procedure as follows: a 50 mL of 0.01 M NaCl were placed into several closed Erlenmeyer flasks and the pH of each flask was adjusted at 3.0, 4.5, 5.6, and 8.0 by adding HCl (0.01 M) or NaOH (0.01 M). Then, 0.2 g Fe-TiO_2/Bent-Fe was added to each flask. The pH_{PZC} is the point where the line of final pH is crossing the line of initial pH.

2.3. Removal Experiments. Experiments were conducted to investigate diazinon removal efficiency by adsorption and photocatalytic degradation of the synthesized materials. In addition, optimal pH, photocatalyst dosage, and light condition were also investigated in the study. In a typical removal experiment, a known dosage of the synthesized photocatalyst (0.25–1 g/L) was transferred to 100 mL of diazinon solution with a distinct concentration (10–50 mg/L) at a certain pH (3–8). The initial pH of solution was adjusted by adding NaOH or HCl (0.1 mol/L) and measured by the pH meter model XT 1200C (Mettler Toledo). After a certain time, the mixture was filtered and the remained diazinon concentrations were measured using a HPLC (Supelco LiChrospher RP-18 column, $250 \times 4.6 \times 5$) coupled to a UV-PDA detector (Shimadzu SPD–M10Avp) at a wavelength of 247 nm. The removal experiment was firstly conducted under dark condition to determine adsorption

capacity of the synthesized material. Then, the visible light was provided to initiate for photocatalytic degradation of diazinon.

3. Results and Discussion

3.1. Material Characteristics

3.1.1. Morphology. Figure 1 shows the SEM images of the synthesized Bent-Fe and Fe-TiO_2/Bent-Fe materials. It can be seen that the synthesized Bent-Fe material existed in form of nanolamella with dominant flake-like morphology and curling edges. The SEM image of the synthesized Fe-TiO_2/Bent-Fe indicated that Fe-TiO_2 particles existed in form of nanospherical particles. The nano-Fe-TiO_2 particles were well-dispersed on the surface of the Bent-Fe layers. This is expected to increase recycling ability of the nano-Fe-TiO_2 photocatalysts after being used for diazinon removal processes. In addition, the deposition of Fe-TiO_2 particles on the surface of the Bent-Fe could increase surface areas of the material, leading to increase in its diazinon removal efficiency. The BET surface area of the synthesized Fe-TiO_2/Bent-Fe (181.13 m^2/g) was greatly higher than that of the Bent-Fe (66.22 m^2/g).

3.1.2. Crystal Phase Structure. Figure 1 shows the XRD patterns of undoped TiO_2, Fe-TiO_2, and Fe-TiO_2/Bent-Fe materials. It can be seen that the anatase and rutile phases were observed in the XRD pattern of the undoped TiO_2 material (JCPDS card No. 65-5714 for anatase and JCPDS card no. 21-1276 for rutile). However, there was only anatase phase in the XRD pattern of the synthesized Fe-TiO_2 photocatalyst. This could be due to the incorporation of Fe dopant into TiO_2 lattice prevented the formation of the rutile phase [33, 34]. There was no peak corresponding to Fe component in the synthesized Fe-TiO_2 material which confirmed that Fe incorporated in the TiO_2 lattice. Figure 1 also shows that the phase structure of the Fe-TiO_2 photocatalyst unchanged when the material was deposited on the Bent-Fe. In addition, a peak corresponding to the montmorillonite phase of the bentonite was also observed in the XRD pattern of the Fe-TiO_2/Bent-Fe material (JCPDS card No. 03-0014) (Figure 2).

3.1.3. Optical Properties. Figure 3 shows the UV-Vis light absorption of the synthesized TiO_2, Bent-Fe, Fe-TiO_2, and Fe-TiO_2/Bent-Fe materials. The UV-Vis absorption spectrum of TiO_2 exhibited an absorption edge at 390 nm [35]. However, the materials did not exhibit any noticeable absorption in the visible region. Bent-Fe also shows little visible light absorption. As compared to the UV-Vis absorption spectra of the TiO_2 and Bent-Fe, that of the Fe-TiO_2, however, not only showed a red shift of the absorption edge but also exhibited higher adsorption ability in the visible region. The band gap structure of the TiO_2 is comprised of a valence band, which is mainly constructed from an O 2p orbital, and a conduction band, which is mainly constructed from an empty Ti 3d orbital. In the Fe-TiO_2, the 3d orbitals of Fe dopant not only affected to the top of the valence band and the bottom of the conduction band of the TiO_2 but also inserted into the TiO_2 lattice structure to create a Fe impurity band under the conduction band and upper the valence band of the TiO_2, formed an optical band gap [33, 36]. Therefore, the photoexcited electrons in the TiO_2 valence band could migrate to the Fe impurity band, and then move from the impurity band to the conduction band via next photon absorption. Thus, the Fe dopant led to decrease in the band-gap energy, recombination rate of photo-excited electrons and holes, as well as increase in visible light absorption of the TiO_2. The UV-Vis absorption spectrum of Fe-TiO_2/Bent-Fe shows that the deposition of the Fe-TiO_2 on the surface of the Bent-Fe extended visible light absorption of the Fe-TiO_2. Krishnan and Mahalingam reported that the increase in visible light absorption was due to the interband transitions i.e., charge transfer transition of interlayer tetrahedral and octahedral atoms in the bentonite material [37].

3.2. Diazinon Removal

3.2.1. Adsorption of Diazinon. First, the effect of contact time on the sorption of diazinon was investigated by adding 0.5 g of the synthesized Fe-TiO_2/Bent-Fe material in 100 mL diazinon solution (16.74 mg/L) at pH 5.6 (natural pH without any adjustment) and room temperature of 25°C. The diazinon adsorption capacities by the synthesized Fe-TiO_2/Bent-Fe are shown in Figure 4(a). It can be seen that the diazinon adsorption capacities increased with increase in contact time up to 30 min and then tend to stabilize with further increase in contact time. It means that the diazinon adsorption by the synthesized Fe-TiO_2/Bent-Fe reaches the equilibrium after 30 min. Based on the obtained results, the experiments, which the contact time was fixed (30 min), were conducted to investigate maximum diazinon adsorption capacity of the synthesized Fe-TiO_2/Bent-Fe. The Langmuir model was applied to calculate the maximum adsorption capacities (Figure 4(b)). It can be seen that the adsorption ability is suitable with the Langmuir model, and the maximum diazinon adsorption capacity (q_{max}) by the synthesized Fe-TiO_2/Bent-Fe was 27.03 (mg/g).

3.2.2. Photocatalytic Degradation of Diazinon. In order to investigate photocatalytic degradation of diazinon, 0.5 g Fe-TiO_2/Bent-Fe material was put in 100 mL diazinon solution (25 mg/L). In the condition, the pH of solution was 5.6 (natural pH without any adjustment). Then, the obtained solution was kept in dark condition for 30 min to get adsorption equilibrium, and then the visible light was provided using a 36 W compact bulb, which could provide visible light in range of 400–700 nm. The diazinon removal results are shown in Figure 5. Under dark condition, an approximately 36.18% diazinon was removed by adsorption of Fe-TiO_2/Bent-Fe material. When visible light was provided, the diazinon was continuously removed by photocatalytic degradation. The synthesized Fe-TiO_2/Bent-Fe could absorb significant amount of incident light to generate huge amount

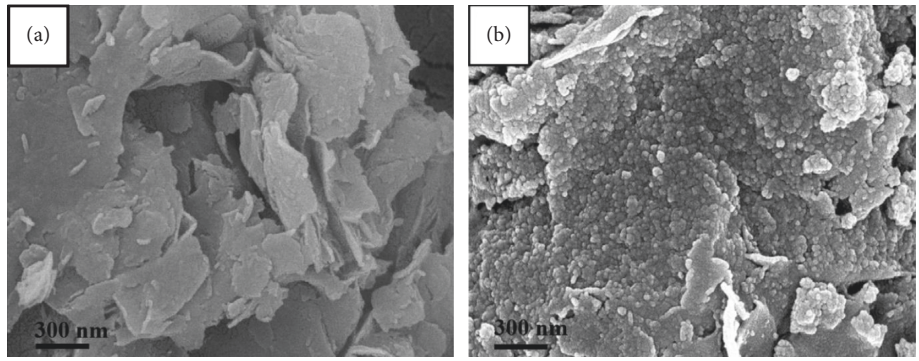

Figure 1: SEM images of the synthesized Bent-Fe and Fe-TiO_2/Bent-Fe materials.

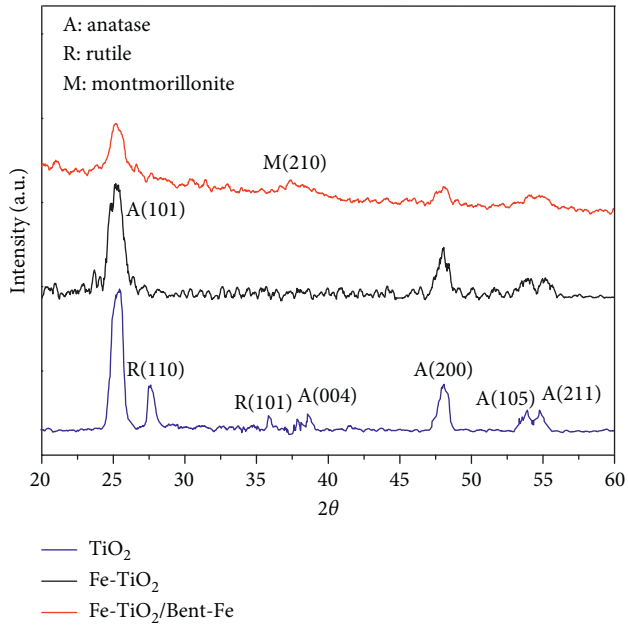

Figure 2: XRD patterns of the synthesized TiO_2, Fe-TiO_2, and Fe-TiO_2/Bent-Fe materials.

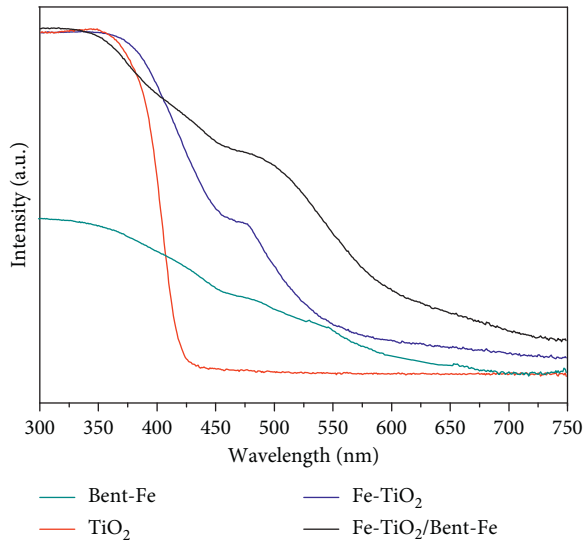

Figure 3: UV-Vis absorption spectra of the synthesized TiO_2, Bent-Fe, Fe-TiO_2, and Fe-TiO_2/Bent-Fe materials.

of electrons and holes. Then, the generated electrons and holes could react with H_2O and O_2, respectively, to produce strong oxidative radicals, including hydroxyl and superoxide anion radicals, for degradation of diazinon into harmless inorganic materials [38–40]. The total diazinon removal by both adsorption and photocatalytic degradation was approximately 58.3%.

3.2.3. Optimal Removal Conditions. The effects of photocatalyst dosages on diazinon removal efficiencies are shown in Figure 6(a). When the photocatalyst dosage was 0.25 g/L, the amount of photocatalyst was not enough for the diazinon removal. The diazinon removal efficiencies increased with increase in photocatalyst dosage up to 1.0 g/L. When the photocatalyst dosages increased, the turbidity of the solution increased. An increased level of suspension turbidity resulted from excessive photocatalyst dosage would block the incident visible light required for the photocatalyst activation [41]. Hence, the photocatalytic degradation efficiency decreased. Thus, the optimal photocatalyst dosage for diazinon removal was 0.5 g/L.

The diazinon removal experiments was conducted under different light conditions including artificial light generated from compact bulb and natural light from solar. The intensity of light from the 36 W compact bulb was 190.985 lux and the intensity of solar light, which was measured in 6 hours of the experiment, varied from 32.500 to 65.200 lux. In the experiments, the photocatalytic dosage, pH, and intimal concentration of diazinon were 0.5 g/L, 5.6, and 25 ppm, respectively. The obtained results are shown in Figure 6(b). The diazinon removal efficiency under natural light generated from solar was 53%, which was slightly lower than that under artificial light generated from compact bulb (58.3%). Thus, the natural light could be suitable used for photocatalytic degradation of diazinon by the synthesized Fe-TiO_2/Bent-Fe material.

Finally, the diazinon removal experiments were conducted at different pH (3.0, 4.5, 5.6 and 8.0) to investigate optimal pH for the process. In the experiments, the photocatalytic dosage and intimal concentration of diazinon were 0.5 g/L and 25 ppm, respectively. The diazinon removal efficiencies at different pH are shown in Figure 6(c). First, the pK_a of diazinon is 2.6, thus diazinon is negatively charged at all the selected pH conditions [2]. Point of zero

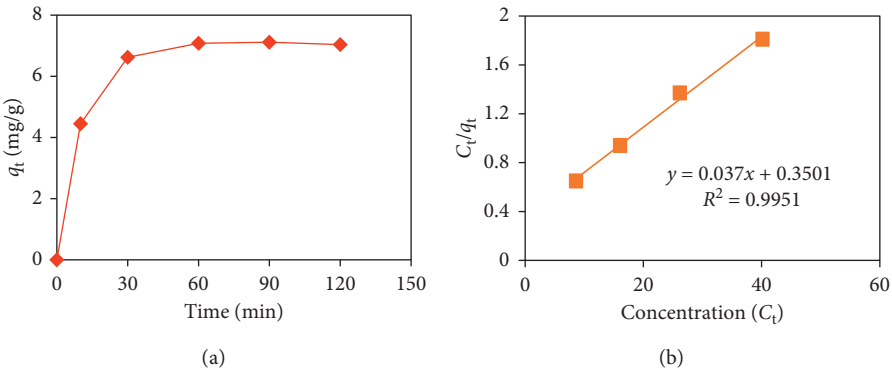

Figure 4: Diazinon adsorption capacities by the synthesized Fe-TiO_2/Bent-Fe (a) and Langmuir model (b).

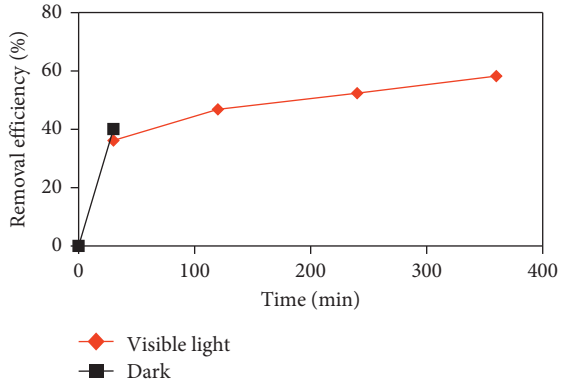

Figure 5: Diazinon removal under dark and visible light conditions.

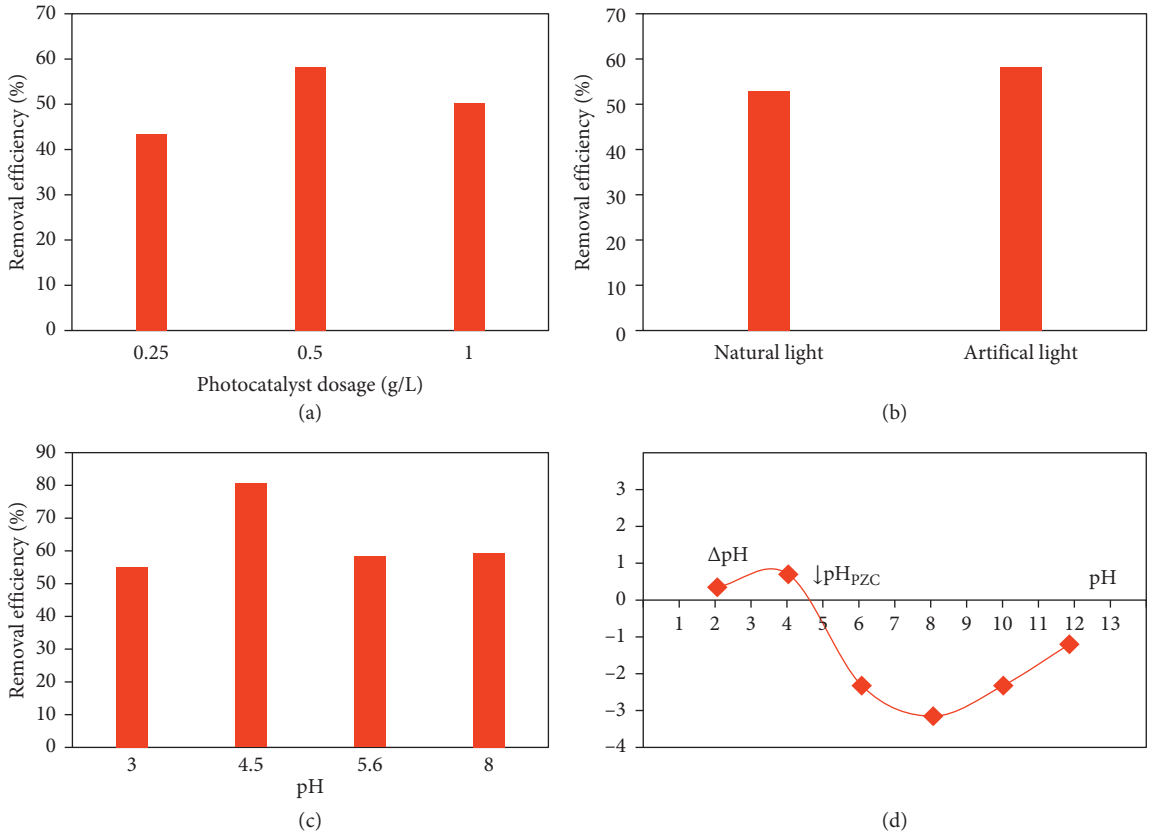

Figure 6: Effects of photocatalyst dosage (a), light sources (b), and pH (c) on diazinon removal efficiencies and zeta potential of the synthesized Fe-TiO_2/Bent-Fe (d).

charge of the synthesized Fe-TiO_2/Bent-Fe material was approximately 4.6 (Figure 6(d)). As expected, an optimal condition can be developed in the pH range between $pK_a^{diazinon}$ and $pH_{zpc}^{Fe-TiO_2/Bent-Fe}$ at which the positively charged Fe-TiO_2/Bent-Fe material and negatively charged diazinon should readily attract each other. At high pH, both diazinon and Fe-TiO_2/Bent-Fe have negative charges. Therefore, electrostatic repulsion between diazinon and Fe-TiO_2/Bent-Fe causes reduced adsorption of diazinon onto material surface, resulting in decreased photocatalytic removal efficiency. Based on the obtained results of this study, pH 4.5 was identified as an optimum condition for the removal of diazinon using Fe-TiO_2/Bent-Fe material. Under optimal conditions, including dosage (0.5 g/L) and pH (4.5), 80.6% diazinon, which the initial concentration was 25 ppm, has been removed by the synthesized Fe-TiO_2/Bent-Fe.

Recycling experiments were conducted to analyze the stability of the prepared photocatalyst during the diazinon removal processes. After being used for diazinon removal for 360 min, the photocatalysts were collected and vacuum dried for 4 h under the dark condition and then used for the diazinon removal experiment. The diazinon removal efficiency by Fe-TiO_2/Bent-Fe in the first and second time of recycle was 76.8 and 69.3%, respectively. The diazinon removal by Fe-TiO_2/Bent-Fe was not significantly changed after recycling, which demonstrated the stability of the photocatalysts during the removal experiments.

4. Conclusion

We successfully used Fe as a dopant to enhance photocatalytic activity of TiO_2. Then, the Fe doped TiO_2 was deposited on bentonite, which was pillared by Fe, to enhance its adsorption and recycling ability in the practical system. The synthesized material exhibited high adsorption ability to remove diazinon. The maximum diazinon adsorption capacity of the synthesized Fe-TiO_2/Bent-Fe was 27.03 mg/g. Even under visible light, the synthesized Fe-TiO_2/Bent-Fe photocatalyst also exhibited high photocatalytic activity for degradation of diazinon. The optimal photocatalyst dosage for removal of diazinon was 0.5 g/L. The natural light generated from solar could be suitable used for diazinon removal by the synthesized Fe-TiO_2/Bent-Fe. Finally, the optimal pH for diazinon removal was 4.5, which is preferred for adsorption of diazinon by the synthesized Fe-TiO_2/Bent-Fe.

Data Availability

The data used to support the findings of this study are included within the article.

Conflicts of Interest

The authors declare that they have no conflicts of interest.

Acknowledgments

This research was funded by the Vietnam National University, Hanoi (VNU), under project number QG.17.27.

References

[1] A. F. Hassan, H. Elhadidy, and A. M. Abdel-Mohsen, "Adsorption and photocatalytic detoxification of diazinon using iron and nanotitania modified activated carbons," *Journal of the Taiwan Institute of Chemical Engineers*, vol. 75, pp. 299–306, 2017.

[2] H. Hossaini, G. Moussavi, and M. Farrokhi, "Oxidation of diazinon in cns-ZnO/LED photocatalytic process: catalyst preparation, photocatalytic examination, and toxicity bioassay of oxidation by-products," *Separation and Purification Technology*, vol. 174, pp. 320–330, 2017.

[3] A.-A. Salarian, Z. Hami, N. Mirzaei et al., "N-doped TiO_2 nanosheets for photocatalytic degradation and mineralization of diazinon under simulated solar irradiation: optimization and modeling using a response surface methodology," *Journal of Molecular Liquids*, vol. 220, pp. 183–191, 2016.

[4] H. Shemer and K. Linden, "Degradation and by-product formation of diazinon in water during UV and UV/H_2O_2 treatment," *Journal of Hazardous Materials*, vol. 136, no. 3, pp. 553–559, 2006.

[5] V. N. Kouloumbos, D. F. Tsipi, A. E. Hiskia, D. Nikolic, and R. B. Breemen, "Identification of photocatalytic degradation products of diazinon in TiO_2 aqueous suspensions using GC/MS/MS and LC/MS with quadrupole time-of-flight mass spectrometry," *Journal of the American Society for Mass Spectrometry*, vol. 14, no. 8, pp. 803–817, 2003.

[6] V. N. Nguyen, D. T. Tran, M. T. Nguyen et al., "Enhanced photocatalytic degradation of methyl orange using ZnO/graphene oxide nanocomposites," *Research on Chemical Intermediates*, vol. 44, no. 5, pp. 3081–3095, 2018.

[7] A. Jonidi-Jafari, M. Shirzad-Siboni, J.-K. Yang, M. Naimi-Joubani, and M. Farrokhi, "Photocatalytic degradation of diazinon with illuminated ZnO-TiO_2 composite," *Journal of the Taiwan Institute of Chemical Engineers*, vol. 50, pp. 100–107, 2015.

[8] S. R. Mirmasoomi, M. Mehdipour Ghazi, and M. Galedari, "Photocatalytic degradation of diazinon under visible light using TiO_2/Fe_2O_3 nanocomposite synthesized by ultrasonic-assisted impregnation method," *Separation and Purification Technology*, vol. 175, pp. 418–427, 2017.

[9] M. Shirzad-Siboni, A. Jonidi-Jafari, M. Farzadkia, A. Esrafili, and M. Gholami, "Enhancement of photocatalytic activity of Cu-doped ZnO nanorods for the degradation of an insecticide: kinetics and reaction pathways," *Journal of Environmental Management*, vol. 186, pp. 1–11, 2017.

[10] E. Rossetto, D. I. Petkowicz, J. H. Z. dos Santos, S. B. C. Pergher, and F. G. Penha, "Bentonites impregnated with TiO_2 for photodegradation of methylene blue," *Applied Clay Science*, vol. 48, no. 4, pp. 602–606, 2010.

[11] A. T. Kuvarega, R. W. M. Krause, and B. B. Mamba, "Evaluation of the simulated solar light photocatalytic activity of N, Ir co-doped TiO_2 for organic dye removal from water," *Applied Surface Science*, vol. 329, pp. 127–136, 2015.

[12] T.-D. Pham and B.-K. Lee, "Advanced removal of *C. famata* in bioaerosols by simultaneous adsorption and photocatalytic oxidation of Cu-doped TiO_2/PU under visible irradiation," *Chemical Engineering Journal*, vol. 286, pp. 377–386, 2016.

[13] N. A. Ramos-Delgado, M. A. Gracia-Pinilla, L. Maya-Treviño, L. Hinojosa-Reyes, J. L. Guzman-Mar, and A. Hernández-Ramírez, "Solar photocatalytic activity of TiO_2 modified with WO_3 on the degradation of an organophosphorus pesticide," *Journal of Hazardous Materials*, vol. 263, pp. 36–44, 2013.

[14] T.-D. Pham, B.-K. Lee, and D. Pham-Cong, "Advanced removal of toluene in aerosol by adsorption and photocatalytic degradation of silver-doped TiO_2/PU under visible light irradiation," *RSC Advances*, vol. 6, no. 30, pp. 25346–25358, 2016.

[15] V. Iliev, D. Tomova, L. Bilyarska, A. Eliyas, and L. Petrov, "Photocatalytic properties of TiO_2 modified with platinum and silver nanoparticles in the degradation of oxalic acid in aqueous solution," *Applied Catalysis B: Environmental*, vol. 63, no. 3-4, pp. 266–271, 2006.

[16] K. Pathakoti, S. Morrow, C. Han et al., "Photoinactivation of *Escherichia coli* by sulfur-doped and nitrogen-fluorine-codoped TiO_2 nanoparticles under solar simulated light and visible light irradiation," *Environmental Science & Technology*, vol. 47, no. 17, pp. 9988–9996, 2013.

[17] H.-Y. Lin and Y.-S. Chang, "Photocatalytic water splitting for hydrogen production on $Au/KTiNbO_5$," *International Journal of Hydrogen Energy*, vol. 35, no. 16, pp. 8463–8471, 2010.

[18] M. Ni, M. K. H. Leung, D. Y. C. Leung, and K. Sumathy, "A review and recent developments in photocatalytic water-splitting using TiO_2 for hydrogen production," *Renewable and Sustainable Energy Reviews*, vol. 11, no. 3, pp. 401–425, 2007.

[19] X. Chen, S. Shen, L. Guo, and S. S. Mao, "Semiconductor-based photocatalytic hydrogen generation," *Chemical Reviews*, vol. 110, no. 11, pp. 6503–6570, 2010.

[20] T.-D. Pham and B.-K. Lee, "Novel integrated approach of adsorption and photo-oxidation using Ag-TiO_2/PU for bio-aerosol removal under visible light," *Chemical Engineering Journal*, vol. 275, pp. 357–365, 2015.

[21] T.-D. Pham and B.-K. Lee, "Cu doped TiO_2/GF for photocatalytic disinfection of *Escherichia coli* in bioaerosols under visible light irradiation: application and mechanism," *Applied Surface Science*, vol. 296, pp. 15–23, 2014.

[22] H. Yan, S. T. Kochuveedu, L. N. Quan, S. S. Lee, and D. H. Kim, "Enhanced photocatalytic activity of C, F-codoped TiO_2 loaded with AgCl," *Journal of Alloys and Compounds*, vol. 560, pp. 20–26, 2013.

[23] X. Xu, X. Zhou, L. Zhang et al., "Photoredox degradation of different water pollutants (MO, RhB, MB, and Cr(VI)) using Fe-N-S-tri-doped TiO_2 nanophotocatalyst prepared by novel chemical method," *Materials Research Bulletin*, vol. 70, pp. 106–113, 2015.

[24] S. M. El-Sheikh, G. Zhang, H. M. El-Hosainy et al., "High performance sulfur, nitrogen and carbon doped mesoporous anatase-brookite TiO_2 photocatalyst for the removal of microcystin-LR under visible light irradiation," *Journal of Hazardous Materials*, vol. 280, pp. 723–733, 2014.

[25] S. Yu, H. J. Yun, Y. H. Kim, and J. Yi, "Carbon-doped TiO_2 nanoparticles wrapped with nanographene as a high performance photocatalyst for phenol degradation under visible light irradiation," *Applied Catalysis B: Environmental*, vol. 144, pp. 893–899, 2014.

[26] T.-D. Pham and B.-K. Lee, "Photocatalytic comparison of Cu- and Ag-doped TiO_2/GF for bioaerosol disinfection under visible light," *Journal of Solid State Chemistry*, vol. 232, pp. 256–263, 2015.

[27] T. D. Pham, B. K. Lee, M. V. Nguyen, and C. H. Lee, "Germicide feasibility of TiO_2/glass fiber and Ag-TiO_2/glass fiber photocatalysts," *Advanced Materials Research*, vol. 864, pp. 518–523, 2012.

[28] H. Feng, M.-H. Zhang, and L. E. Yu, "Hydrothermal synthesis and photocatalytic performance of metal-ions doped TiO_2," *Applied Catalysis A: General*, vol. 413-414, pp. 238–244, 2012.

[29] R. Djellabi, M. F. Ghorab, G. Cerrato et al., "Photoactive TiO_2-montmorillonite composite for degradation of organic dyes in water," *Journal of Photochemistry and Photobiology A: Chemistry*, vol. 295, pp. 57–63, 2014.

[30] L. M. Martínez T, M. I. Domínguez, N. Sanabria et al., "Deposition of Al-Fe pillared bentonites and gold supported Al-Fe pillared bentonites on metallic monoliths for catalytic oxidation reactions," *Applied Catalysis A: General*, vol. 364, no. 1-2, pp. 166–173, 2009.

[31] M. Yurdakoç, M. Akçay, Y. Tonbul, F. Ok, and K. Yurdakoç, "Preparation and characterization of Cr- and Fe-pillared bentonites by using $CrCl_3$, $FeCl_3$, $Cr(acac)_3$ and $Fe(acac)_3$ as precursors," *Microporous and Mesoporous Materials*, vol. 111, no. 1–3, pp. 211–218, 2008.

[32] J. Chen and L. Zhu, "Comparative study of catalytic activity of different Fe-pillared bentonites in the presence of UV light and H_2O_2," *Separation and Purification Technology*, vol. 67, no. 3, pp. 282–288, 2009.

[33] A. Eshaghi and H. Moradi, "Optical and photocatalytic properties of the Fe-doped TiO_2 nanoparticles loaded on the activated carbon," *Advanced Powder Technology*, vol. 29, no. 8, pp. 1879–1885, 2018.

[34] G. Wei, L. Wei, Y. Chen et al., "Magnetic coupling and electric transport in Nb, Fe co-doped rutile TiO_2 epitaxial films," *Journal of Alloys and Compounds*, vol. 695, pp. 2261–2265, 2017.

[35] X. Cao, S. Luo, C. Liu, and J. Chen, "Synthesis of bentonite-supported Fe_2O_3 -Doped TiO_2 superstructures for highly promoted photocatalytic activity and recyclability," *Advanced Powder Technology*, vol. 28, no. 3, pp. 993–999, 2017.

[36] A. A. Isari, A. Payan, M. Fattahi, S. Jorfi, and B. Kakavandi, "Photocatalytic degradation of rhodamine B and real textile wastewater using Fe-doped TiO_2 anchored on reduced graphene oxide (Fe-TiO_2/rGO): characterization and feasibility, mechanism and pathway studies," *Applied Surface Science*, vol. 462, pp. 549–564, 2018.

[37] B. Krishnan and S. Mahalingam, "Ag/TiO_2/bentonite nanocomposite for biological applications: synthesis, characterization, antibacterial and cytotoxic investigations," *Advanced Powder Technology*, vol. 28, no. 9, pp. 2265–2280, 2017.

[38] T.-D. Pham and B.-K. Lee, "Selective removal of polar VOCs by novel photocatalytic activity of metals co-doped TiO_2/PU under visible light," *Chemical Engineering Journal*, vol. 307, pp. 63–73, 2017.

[39] T.-D. Pham, B.-K. Lee, and C.-H. Lee, "The advanced removal of benzene from aerosols by photocatalytic oxidation and adsorption of Cu-TiO_2/PU under visible light irradiation," *Applied Catalysis B: Environmental*, vol. 182, pp. 172–183, 2016.

[40] T.-D. Pham and B.-K. Lee, "Novel adsorption and photocatalytic oxidation for removal of gaseous toluene by V-doped TiO_2/PU under visible light," *Journal of Hazardous Materials*, vol. 300, pp. 493–503, 2015.

[41] D. Kanakaraju and S. P. Wong, "Photocatalytic efficiency of TiO_2-biomass loaded mixture for wastewater treatment," *Journal of Chemistry*, vol. 2018, Article ID 4314969, 14 pages, 2018.